Proceedings of the ASME 2018 Conference on Smart Materials, Adaptive Structures and Intelligent Systems
SMASIS2018
September 10-12, 2018, San Antonio, Texas, USA

SMASIS2018-8121

LINEAR PARAMETER VARYING MODELING AND ESTIMATION OF A SMA WIRE ACTUATOR

Kyle Kubik
Department of Mechanical Engineering
Auburn, Alabama, USA

Austin Gurley[1]
Deft Dynamics
Birmingham, Alabama, USA

David Beale
Department of Mechanical Engineering
Auburn, Alabama, USA

Amanda Skalitzky
Department of Mechanical Engineering
Auburn, Alabama, USA

ABSTRACT

Shape Memory Alloys (SMAs) actuators operate via a nonlinear and hysteretic relationship between input power and mechanical motion. This nonlinearity presents a serious challenge when developing methods for controlling these actuators. Because this hysteresis and nonlinearity is caused by the crystal phase transformation however, the SMA constitutive and kinetic models can be written in Linear Parameter Varying (LPV) form, with the partial derivative of crystal phase fraction with respect to temperature as the varying parameter. This allows a SMA system to be written in a state-space format where the coefficients in the state matrices vary as a function of the state variables, allowing for the application of powerful linear system analysis tools to this model without simplifying assumptions. This LPV model can then be used to create an estimator for the system, allowing for real-time approximations of the system states, including temperature and phase fraction. This paper presents the derivation of one such LPV model and explores its ability to accurately represent a physical SMA actuator system by comparison with an instrumented SMA muscle system.

INTRODUCTION

SMA actuators boast many benefits over traditional actuator technologies including lower cost and complexity, higher specific strength, and silent actuation. They have yet to see widespread adoption, however, partially due to the challenges posed by the nonlinearity of the shape memory effect to controls design. To effectively use SMA actuators, it is critical to create an accurate model of the material's behavior that is simple enough to be effective as a base for the design of control laws. Among the many discovered SMAs, Nitinol (NiTi) is by far the most popular material used for actuator design, primarily due to its relatively low cost and high availability. Drawing NiTi into fine wires makes it possible to heat the material by passing an electric current through it, a beneficial property for the design of lightweight actuators. For many actuation tasks, the NiTi wire actuator is the preferable alloy and form and as such will be the focus of this paper.

The actuation of a NiTi wire actuator is driven by affecting the material's phase fraction, which is a function of stress and temperature, and ultimately affects the overall strain of the wire. Therefore, it is important when designing control systems for these actuators to consider these states. The accuracy of a control solution could be greatly increased by adding a measurement of stress or temperature to the system. Unfortunately, it is not often practical to directly measure the stress or temperature of a typical NiTi wire actuator without greatly increasing its cost and size. For this reason, it is useful to instead estimate these states within the wire, as we have done here.

This paper presents an introduction to the shape memory effect, followed by a review of common phenomenological models used to describe the effect. A practical thermo-mechanical model is then developed with the focus of a real-time controls application. Next, the model incorporated into a generalized mechanical system and presented in a LPV State Space form. From this LPV model, a state estimator is

[1] Corresponding author

formulated which demonstrates the ability to accurately estimate and track both the phase fraction and the temperature of the actuator with a strain measurement and known power input. Finally, the state estimator is implemented on a physical SMA actuator system in conjunction with a simple PID controller as a method of tracking and limiting the temperature of the actuator to prevent damage from overheating.

BACKGROUND

In Nitinol, the shape memory effect is driven by the transition between two distinct crystalline phases. 'Austenite'- a short and stiff structure, and 'Martensite' - a comparatively long and flexible structure. The material experiences reversible crystalline transformation because of changes of stress or temperature. At low temperatures or high stresses, the material is dominated by Martensite crystals, and can experience a reversable strain of around 4%. By applying heat or reducing the stress on the material, the martensite crystals transition to austenite. At low stress and temperatures, two additional crystalline phases can be observed within the material typically referred to as 'Twinned Martensite', a compacted form of the Martensite phase, and 'R-phase', which competes with Martensite within the material. For actuator design, it is practical to operate outside the stress range where these phases form, and as such they will not be explored in detail here. An approximate representation of the phase diagram for NiTi is presented in figure 1.

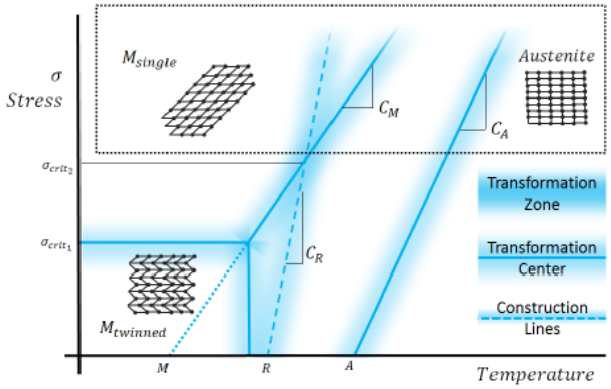

Figure 1: Complete SMA phase diagram. SMA wire actuators are designed to operate in the boxed region

An initial simplifying assumption is that our NiTi Wire actuator is under a sufficient amount of pre-load to prevent the formation of Twinned Martensite (the area inside a dotted rectangle in figure 1). This simplifies the phase diagram significantly, and eliminates the 'R-phase' region of the material which can complicate the electrical characteristics of the wire [1]. The new phase diagram is shown in figure 2.

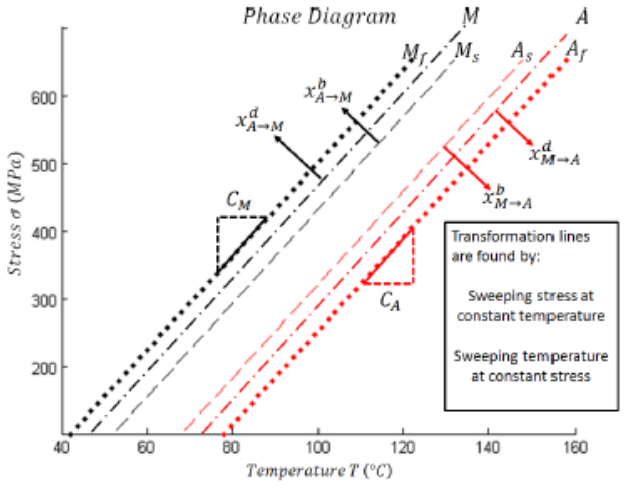

Figure 2: The SMA phase diagram for stress above 100MPa

Typically, the values which describe the transformation regions are found experimentally, for example by placing the material within a Differential Scanning Calorimeter (DSC) which measures heat flow vs. temperature, as can be seen in figure 3.

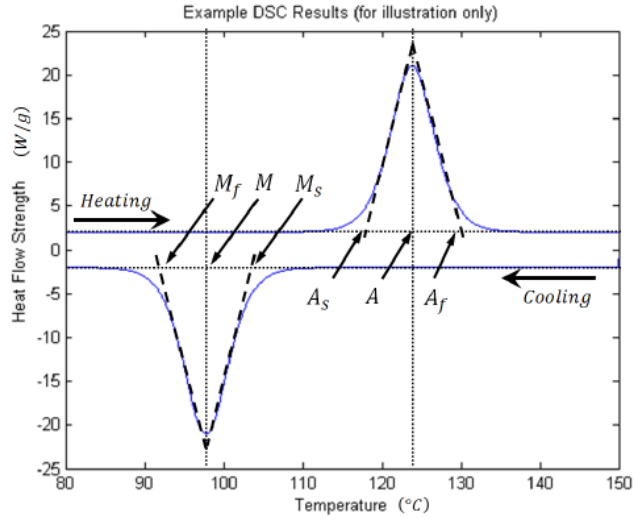

Figure 3: Typical (simulated) DSC experiment shows temperature induced phase change from M to A, and back to M from A (with constant macroscopic stress)

Many methods have been presented for the phenomenological modelling of Nitinol, varying from one-dimensional analysis [2, 3] to multi-dimensional mechanics [4, 5, 6, 7] and finite element approximations [8, 9, 10]. For the purposes of dynamic system modelling, it is preferable to utilize a one-dimensional model, which offers the best compromise of simplicity and accuracy. Especially in the case of NiTi Wire actuators, a one-dimensional assumption is acceptable, this can be seen in work comparing common models to experimental data [11, 12].

Constitutive Model

Tanaka [13] presents the following equation for the constitutive relationship between stress, strain, temperature, and phase fraction within the material:

$$\dot{\sigma} = E(\xi)\dot{\epsilon} - \Theta(\xi)\dot{T} + \Omega(\xi)\dot{\xi} \tag{1}$$

Where E is the Elastic Modulus, Θ is the Coefficient of Thermal Expansion, and Ω is the 'transformation tensor', all of which are functions of the Martensite fraction (ξ). Liang & Rodgers [14] note that this model is only consistent for the following form of $\Omega(\xi)$ where ϵ_L is the maximum shape-memory strain with no stress

$$\Omega(\xi) = \epsilon_L E(\xi) \tag{2}$$

Brinson and Huang [2] pose that the constitutive model is most meaningfully rearranged into the following 'strain decomposition' form.

$$\epsilon = C(\xi)\sigma + \epsilon_L\xi + C(\xi)\Theta(\xi)(T - T_0) \tag{3}$$

$$C(\xi) = \frac{1}{E(\xi)} = \frac{(1-\xi)}{E_A} + \frac{\xi}{E_M} \tag{4}$$

Additionally, the effect of thermal expansion is small compared to the shape memory effect, which is also dependent on temperature. For this reason, the constitutive model is often simplified further to [15]

$$\epsilon = C(\xi)\sigma + \epsilon_L\xi \tag{5}$$

Phase Transformation

Next, it is important to determine criteria for when the phase change is occurring. These transformation conditions are typically based on the phase diagram and are a function of the stress and temperature of the material. Several condition sets have been summarized by Elahinia [16, 17]. Tanaka first used the transformation conditions [13]

$$if \begin{Bmatrix} \dot{\sigma} < 0 \; and \; \sigma \leq -(T - A_s)C_A \\ \dot{\sigma} > 0 \; and \; \sigma \geq (T - M_s)C_M \end{Bmatrix} then \begin{Bmatrix} \xi_{M\to A} \\ \xi_{A\to M} \end{Bmatrix} \tag{6}$$

Where A_s and M_s denote the Austinite and Martensite Start temperatures, C_A and C_M denote the slopes of the Austenite and Martensite transformation lines, and $\xi_{M\to A}$ and $\xi_{A\to M}$ are used to denote the direction that ξ is transforming (from Martensite to Austenite, or from Austenite to Martensite respectively).

Many models bound the transformation to lie only within the start and finish conditions [14, 16, 17, 18]. While this is physically consistent with thermodynamics, it can be seen from DSC experiments that the transformation is continuous at the start and finish conditions. Considering this, models for transformation criteria can be simplified to depend only on the direction of temperature and stress change [19, 20, 21]

$$if \begin{Bmatrix} \dot{T} - \dfrac{\dot{\sigma}}{C_A} > 0 \\ \dot{T} - \dfrac{\dot{\sigma}}{C_M} < 0 \end{Bmatrix} then \begin{Bmatrix} \xi_{M\to A} \\ \xi_{A\to M} \end{Bmatrix} \tag{7}$$

Transformation models using the above criteria can use any function of stress and temperature which is bounded between 0 and 1 for all values of stress and temperature to describe the changing phase fraction. The most common model used with these criteria is the logistic function [19, 20, 22] which can be written as

$$while \begin{Bmatrix} \xi_{M\to A} \\ \xi_{A\to M} \end{Bmatrix}, \begin{Bmatrix} \xi = \dfrac{\xi_M}{1 + \exp\left(k\left(T - \dfrac{\sigma}{C_A} - A\right)\right)} \\ \xi = \dfrac{1 - \xi_A}{1 + \exp\left(-k\left(T - \dfrac{\sigma}{C_M} - M\right)\right)} + \xi_A \end{Bmatrix} \tag{8}$$

Where k is a fitting parameter determined from DSC testing that determines the width of the transformation band, and A and M denote the temperature for the center of the Martensite and Austenite transformation regions at zero stress. ξ_A and ξ_M are 'history variables' which track the extent of the phase transformation and allow for the reversal of the transformation while the phase fraction is not at 0 or 100%.

$$while \begin{Bmatrix} \xi_{M\to A} \\ \xi_{A\to M} \end{Bmatrix}, \begin{Bmatrix} \xi_A = \xi \\ \xi_M = \xi \end{Bmatrix} \tag{9}$$

Heat Transfer

The most convenient way to actuate a NiTi wire actuator is to heat it through resistive heating and allow it to cool in open air. In this configuration, the energy balance equation of the actuator can be written as:

$$mc_p\dot{T} - m\Delta H\dot{\xi} = P + AL\sigma\epsilon_L\dot{\xi} - hA_s(T - T_\infty) \tag{10}$$

where P is electrical power, m is the mass of the wire, c_p is specific heat, ΔH is the latent heat of transformation, h is the convective heat transfer coefficient, A_s is the surface area of the wire, and T_∞ is the ambient air temperature. The primary source of energy is electrical power with deformation energy also included. Energy is stored in the material as sensible and latent heat, and released by convection. Other sources and sinks of energy are considered negligible in this case. Some models for heat transfer also include radiation as an energy sink [23], but its

effect is small compared to convection in many cases and as such is ignored.

THERMO-MECHANICAL MODEL

Using the models presented in the previous section as a starting point, it is useful to simplify the equations with the purpose of controlling an SMA actuator in mind. The final model must compromise between accuracy and computational efficiency. Previous estimation models have been developed by Crews and Smith which can estimate various properties of a SMA material with impressive accuracy [24], but the complexity of the model makes it difficult for use in real-time control applications. Another model, developed by Elahinia and Ashrafiuon [25] can quickly predict the steady state value of strain and temperature of a wire, but lacks accuracy in its transient response. The following model was developed with the intention of being a middle ground between these two models, a lightweight model with acceptable accuracy at all points. We begin by simplifying the strain constitutive model.

$$\epsilon = \frac{\sigma}{E} + \epsilon_L \xi + \Theta T \tag{11}$$

Where E is the elastic modulus, ϵL is the maximum shape memory strain, and Θ is the coefficient of thermal expansion. Because the thermal expansion is small compared to the other strain components, it is usually ignored. For controller design, the elastic modulus is considered to be constant. It is valuable now to rearrange such that stress rate is the dependent variable, the first important constitutive equation:

$$\dot{\sigma} = E\dot{\epsilon} + E\epsilon_L \dot{\xi} \tag{12}$$

The second equation governs the hysteresis of the crystal phase fraction. It is useful to characterize the transformation with a population growth equation to represent the propagation of the crystal transformation through the material. We chose the piecewise logistic function which accurately models the hysteresis, with enhancements that ensure the model is continuous. During simulation the Martensite phase fraction hysteresis behavior can be represented using conditions for transformation derived from the phase diagram:

$$if\left(\dot{T} - \frac{\dot{\sigma}}{\alpha} > 0\right)\begin{cases} \xi = \dfrac{\xi_M}{1 + \exp\left(k\left(T - \frac{\sigma}{\alpha} - A\right)\right)} \\ \xi_A = (1-\xi)(1 + \exp\left(-k\left(T - \frac{\sigma}{\alpha} - M\right)\right) \\ \dfrac{\partial \xi}{\partial T} = k\left(\dfrac{\xi^2}{\xi_M} - \xi\right) \end{cases}$$

$$if\left(\dot{T} - \frac{\dot{\sigma}}{\alpha} < 0\right)\begin{cases} \xi = \dfrac{1-\xi_A}{1 + \exp\left(-k\left(T - \frac{\sigma}{\alpha} - M\right)\right)} + \xi_A \\ \xi_M = \xi(1 + \exp\left(k\left(T - \frac{\sigma}{\alpha} - A\right)\right) \\ \dfrac{\partial \xi}{\partial T} = k\left(\dfrac{(1-\xi)^2}{\xi_A} - (1-\xi)\right) \end{cases} \tag{13}$$

$$\frac{\partial \xi}{\partial \sigma} = -\frac{1}{\alpha}\frac{\partial \xi}{\partial T} \tag{14}$$

Where A (M) is the temperature for the center of Austenite (Martensite) transformation with no stress, the slope of the transformation centerline for Austenite and Martensite (C_A and C_M respectively) are considered equal and denoted by α, k determines the width (or distribution) of the transformation region, and $\xi_{A(M)}$ denotes the extent of the previous transformation (it drives the hysteresis). The time rate of change of ξ is computed using the partial derivatives:

$$\dot{\xi} = \frac{\partial \xi}{\partial T}\dot{T} + \frac{\partial \xi}{\partial \sigma}\dot{\sigma} \tag{15}$$

In addition to the material model, it necessary to model the energy balance between electrical heating power ($P = VI$), wire temperature, and ambient air temperature:

$$mc_p\dot{T} = P + m\Delta H\dot{\xi} + AL\sigma\epsilon_L\dot{\xi} - hA_s(T - T_\infty) \tag{16}$$

Where m is the SMA mass, c_p the specific heat, h is the heat transfer coefficient, ΔH is the latent heat of transformation, and As is the wire surface area. Many SMA materials have a response that is nearly independent of stress. Also, in many applications the stress of preloading is large compared to dynamic load variations. In these cases, the material model is simplified, when designing controllers, to assume stress cannot affect the phase fraction (there is no super-elastic behavior), resulting in the following simplification to equation (15):

$$\dot{\xi} = \frac{\partial \xi}{\partial T}\dot{T} \tag{17}$$

This reduces the complexity of (16) greatly:

$$\left(mc_p - m\Delta H\frac{\partial \xi}{\partial T}\right)\dot{T} = P - hA_s(T - T_\infty) \tag{18}$$

Notice that the effect of transformation effectively changes the thermal mass in an otherwise linear ODE. Equations (12), (13), (17), and (18) provide a complete thermo-mechanical model for controls design and analysis.

It is acceptable to ignore the effect of stress on the phase fraction when an SMA actuator is used to control a reasonable payload, because the temperature is the primary driver of phase change. This can be seen in a simple demonstration where a constant power is applied to heat an actuator that is driving a spring-mass-damper (Figure 4). It was shown in (15) that phase change rate is comprised of stress and temperature components. In a simulation, the phase change rate is tracked as well as these two components. The temperature component (red) has a much larger effect than stress (blue); the total phase change (black) is almost equal to the temperature component alone.

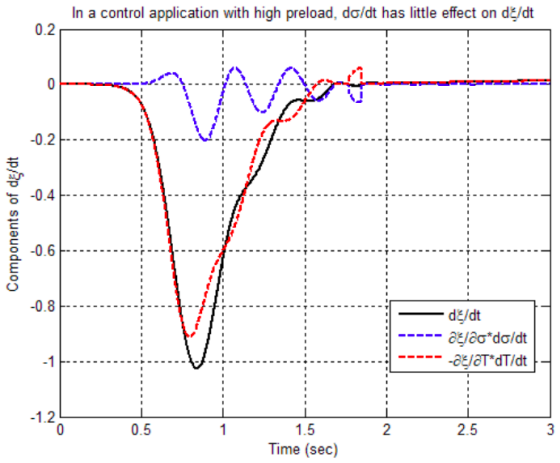

Figure 4: The phase change rate (black) is comprised of stress (blue) and temperature (red) components. Temperature is the primary driver of phase change for actuators, not stress

SYSTEM MODEL

Consider an SMA wire controlling the position of a linear spring-mass-damper system with external preload or disturbance force. This general model can represent many physical systems such as robot arm joints, linear positioning systems, etc. Based on the simplified equations just reviewed, the conventional and physical view of the SMA actuator control system is shown in Figure 5. This model has an SMA wire connected between a fixed wall and the spring-mass-damper plant. The actuation arises from change in the internal state of the material.

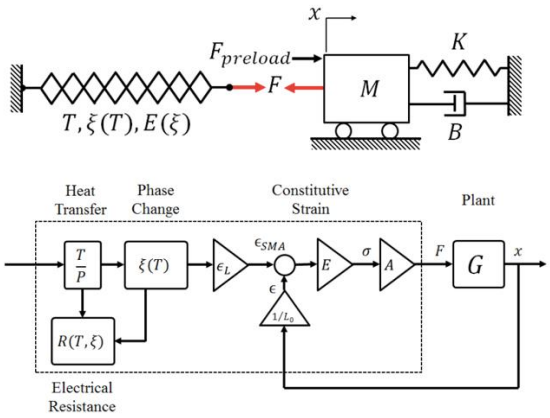

Figure 5: A system model which isolates the SMA actuator from the plant

However, the change of internal material states is not often intuitive. For clarity, the system can be reformed into an equivalent mechanical system as in Figure 6. This model breaks the single SMA material with internal material changes into two parts; the inelastic 'shape memory strain', and an elastic spring. This view of the system makes it clear where the nonlinearity occurs (between temperature change and crystal phase fraction), and eliminates the need to keep stress as a state variable.

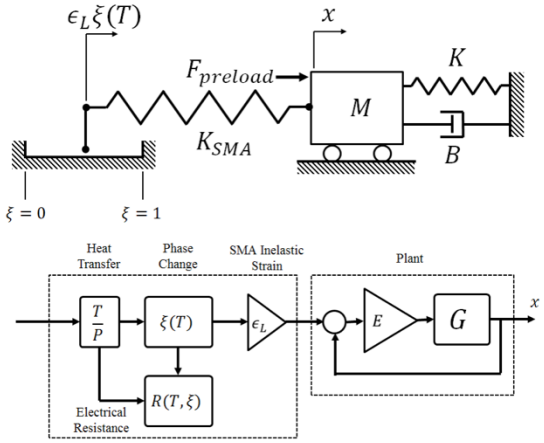

Figure 6: An equivalent system model presented in a form useful for controller design

The full system model can now be presented in LPV state space form. The SMA actuator is represented as an elastic spring with a spring rate of K_{SMA} being pushed by the shape-memory strain ($\epsilon_L \xi$). The model is of the form

$$\begin{Bmatrix} \dot{x} \\ \ddot{x} \\ \dot{\xi} \\ \dot{T} \end{Bmatrix} = A \begin{Bmatrix} x \\ \dot{x} \\ \xi \\ T \end{Bmatrix} + B * P$$

$$A = \begin{bmatrix} 0 & 1 & 0 & 0 \\ -\frac{K + K_{SMA}}{M} & -\frac{B}{M} & \frac{K_{SMA} L \epsilon_L}{M} & 0 \\ 0 & 0 & 0 & -\frac{hA_s}{Q}\frac{\partial \xi}{\partial T} \\ 0 & 0 & 0 & -\frac{hA_s}{Q} \end{bmatrix}$$

$$B = \begin{bmatrix} 0 \\ 0 \\ \frac{\partial \xi}{\partial T}/Q \\ 1/Q \end{bmatrix}$$

$$Q \equiv mc_p - m\Delta H \frac{\partial \xi}{\partial T} \qquad (19)$$

The only varying parameter is the partial derivative of phase fraction with respect to temperature. This parameter takes on a value in the range

$$-\frac{k}{4} < \frac{\partial \xi}{\partial T} < 0$$

This parameter has a minimum in the center of phase change where a small change in temperature greatly affects the phase fraction. The parameter is near zero when the temperature is far from the transformation range, and when the hysteretic phase change direction has recently reversed. This varying parameter affects the apparent dynamics of the system greatly as can be seen in a 'snapshot' pole-zero map in figure 7. When $\frac{\partial \xi}{\partial T}$ is near zero (far from the transformation region), the pole of the temperature response (which moves along the real axis) is at its fastest. Inversely, when $\frac{\partial \xi}{\partial T}$ is near $\frac{-k}{4}$ (at the center of the transformation region) the temperature response of the material is slow, as the phase transformation absorbs the incoming power.

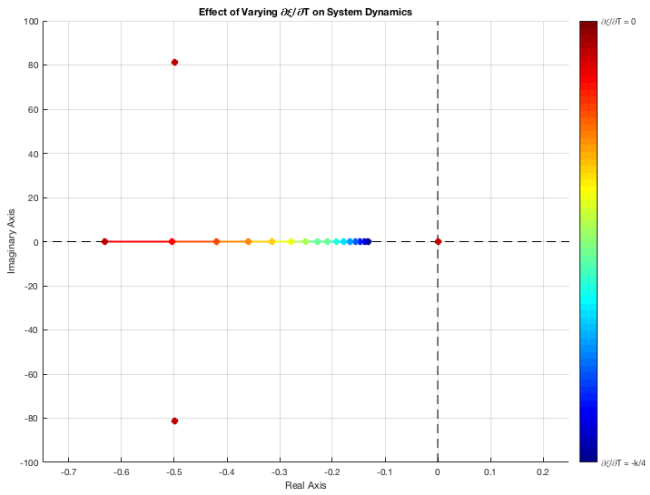

Figure 7: Pole locations for the given system model

Consider a 'snap-shot' of this model where $\partial\xi/\partial T$ is frozen (though not rigorous in general, this is fair since the nonlinearity is first order with negative definite eigenvalue [26]). The model is observable, but not controllable. The lack of controllability can be seen in two ways. Mathematically, the third and fourth rows of A are clearly not linearly independent. This leads to a controllability matrix with rank 3 – proving the system is not controllable for any value of $\partial\xi/\partial T$. As a practical interpretation, it is easy to see that we cannot drive the system to have both a unique temperature and unique phase fraction simultaneously because temperature and phase fraction are constitutively coupled. The system can, however, be controlled with a reduced order model.

STATE ESTIMATOR

The LPV model was used to create a state estimator. This estimator has gains designed based on pole placement, with the estimator time constants selected to be more than ten times faster than the closed-loop system behavior, so that the estimator does not interfere with the control transient response. The estimator is implemented using:

$$\dot{\hat{x}} = \bar{A}\hat{x} + \bar{B}u + L(y - \hat{y}), \qquad \hat{y} = \bar{C}\hat{x}$$

or

$$\dot{\hat{x}} = (\bar{A} - L\bar{C})\hat{x} + \bar{B}u + Ly$$

If the assumed model $(\bar{A}, \bar{B}, \bar{C})$ and the exact system (A, B, C) coincide, then the dynamics of the error are determined by:

$$e \equiv x - \hat{x}$$
$$\dot{e} \equiv \dot{x} - \dot{\hat{x}}$$
$$\dot{e} = (A - LC)e$$

Consider an example SMA wire actuator of 0.125mm diameter. The natural pole of the temperature response is $\lambda_T = -0.7228$ (1/s). The estimator is designed using poles that are faster than ten times this: $Real(\lambda_{est}) < -7.228$. In the simulations

presented below, estimator closed loop poles were chosen to be negative real, all faster than this minimum speed.

In practice, the estimator gain is too complex to recompute (on a microcontroller) after each sample while the controller is running. However, the state transition matrix A and input gain B can only be updated if $\partial\xi/\partial T$ is known or is estimated. There are three ways to address this: by using a constant matrix that represents the average properties, by switching between a few controllers based on the region of operation, or by continually adjusting the state model as the system varies. The first method is only reliable for the states that are not derivatives of nonlinear terms – so it can track the position, speed, and phase fraction accurately, but not temperature. However, using the gain scheduled estimator, the temperature and all other states are accurately recovered after initial offsets are removed by the estimator. A simple (poorly tuned) PI controller is used to demonstrate both estimators in simulation. The complete non-linear thermomechanical models presented at the beginning of the paper were used as the physical system, and the LPV model developed in this chapter was used for the estimator design. Figure 8 demonstrates the estimator using average properties, and Figure 9 demonstrates the gain-scheduled estimator. Both estimators accurately track the position and phase fraction. Both struggle to track temperature when far from the transformation region (where ξ is changing and $\partial\xi/\partial T$ is near zero). The average constant-coefficient model cannot accurately determine temperature. The gain scheduled controller can accurately track temperature once initial errors are eliminated, as expected.

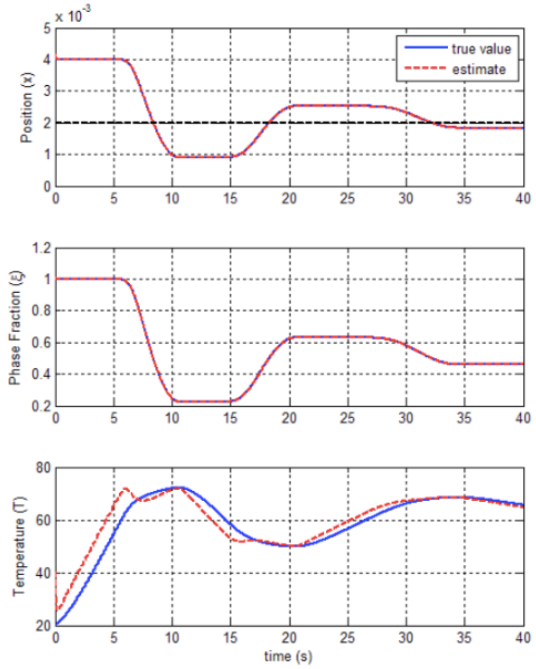

Figure 8: Estimator using average properties accurately estimates phase fraction but does not accurately track the temperature due to ignored nonlinearities

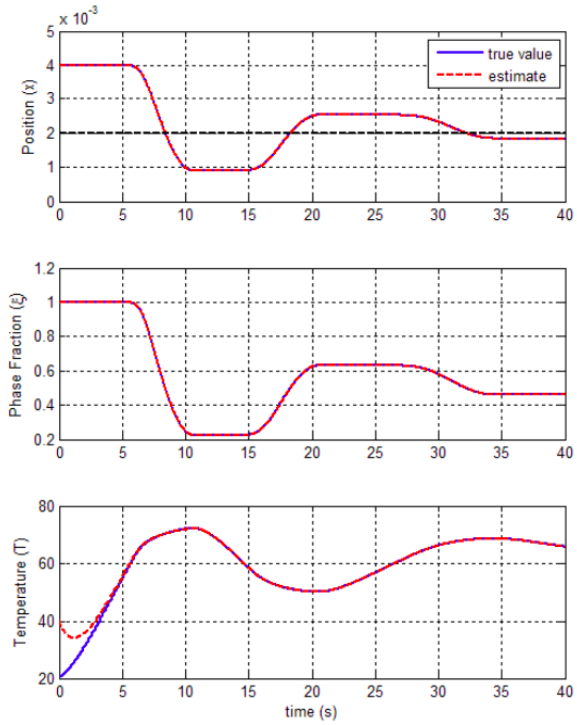

Figure 9: Estimator using gain-scheduling still struggles when far from the transformation region, but quickly tracks all state variable during transients

APPLICATION

The state estimator was implemented in conjunction with a position-based PID controller to drive the angle of a simple robotic arm from 30 to 60 degrees (Figure 10). The only sensor attached to the device was an angular potentiometer for measuring the position of the arm, while the power provided to the wire was the controlled input. After a few cycles to ensure that the PID control was tracking the reference appropriately, a physical stop was added into the path of the arm at about 45 degrees. To overcome the error between position and the reference, the PID controller tries to continue increasing the power to the wire, thus driving its temperature into a dangerous range for the wire and the components around it. However, when the estimated temperature reaches a defined limit, the power output of the controller is limited to prevent the wire from getting any hotter. The entire process is shown in Figure 11. This temperature 'watchdog' allows the device to operate across a wide variety of speeds and loads without the risk of damaging the NiTi wire actuator or any of the surrounding components.

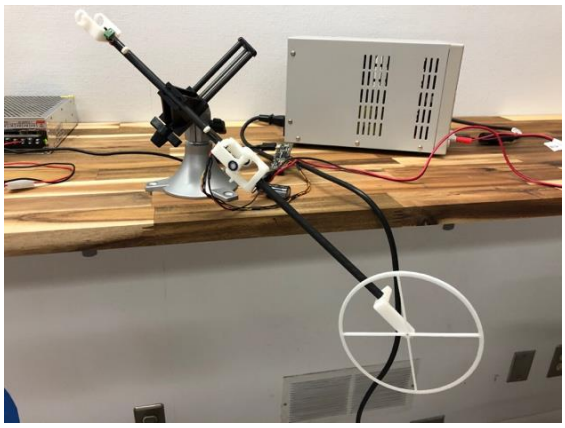

Figure 10: Robotic arm device controlled by a NiTi wire actuator

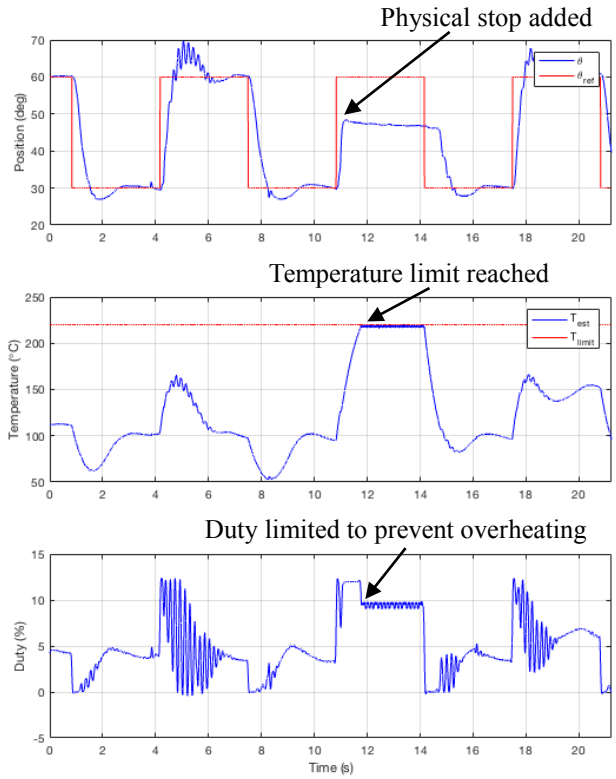

Figure 11: PID controller with temperature estimation. A physical stop is added to the system at 11 seconds

CONCLUSION

Presented here is a linear parameter varying state space model for the simulation of NiTi wire actuators. While this model is not controllable, it is fully observable, and as such is useful for the creation of a state estimator which can predict the phase fraction and temperature of the wire. Both states are difficult to measure for thin NiTi wires, especially in the context of actuator design, where adding additional sensors to the system is not ideal. As such, the ability to approximate these states allows for more complex and accurate control methods without additional cost to actuator design.

In practice, the estimator uses a gain calculated from average properties running alongside a main control law on a microcontroller. It can quickly and accurately estimate phase fraction, and provides a reasonable approximation of temperature. These approximations can be utilized to augment the control of the system, for instance by limiting the temperature of the wire to a safe level.

The presented model ignores some nonlinearities of the system that are largely affected by unexpected disturbances to the system, such as a change in h due to changing air velocity, or large changes in the stress acting on the material. An improved model could account for these disturbances and the states could be estimated via an Extended Kalman Filter or other nonlinear estimation techniques.

REFERENCES

[1] S. Furst, J. Crews and S. Seelecke, "Stress, Strain, and Resistance Behavior of Two Opposing Shape Memory Actuator Wires for Resistance Based Self-Sensing Applications," *Intelligent Material Systems and Structures,* vol. 24, no. 16, pp. 1951-1968, 2013.

[2] L. Brinson and M. Huang, "Simplifications and Comparisons od Shape Memory Alloy Constitutive Models," *Journal of Intelligent Material Systems and Structures,* vol. 7, pp. 108-114, 1996.

[3] A. Pavio and A. Savi, "An Overview of Constitutive Models for Shape Memory Alloys," *Mathematical Problems in Engineering,* vol. 2006, pp. 1-30, 2006.

[4] J. G. Boyd and D. C. Lagoudas, "A Thermodynamical Constitutive Model for Shap Memory Materials. Part II. The SMA Composite Material," *International Journal of Plasticity,* vol. 12, no. 7, pp. 843-873, 1996.

[5] J. G. Boyd and D. C. Lagoudas, "A Thermodynamical Constitutive Model for Shape Memory Materials. Part I. The Monolithic Shape Memory Alloy," *International Journal of Plasticity,* vol. 12, no. 7, pp. 805-842, 1996.

[6] D. Lagoudas, D. Hartl, Y. Chemisky, M. Luciano and P. Popov, "Constitutive Model for the Numerical Analysis of Phase Transformation in Polycrystalline Shape Memory Alloys," *International Journal of Plasticity,* vol. 32, no. 33, pp. 155-183, 2012.

[7] A. Duval, M. Haboussi and T. Ben Zineb, "Modelling of Localization and Propogation of Phase Transformation in Superelastic SMA by a Gradient Nonlocal Approach".

[8] P. Junker, "An Accurate, Fast and Stable Material Model for Shape Memory Alloys," *Smart Materials and Structures,* vol. 23, pp. 1-15, 2014.

[9] F. Auricchino and E. Sacco, "A Temperature-Dependent Beam for Shape-Memory Alloys: Constitutive Modelling, Finite-Element Implementation and Numerical

Simulations," *Computer Methods in Applied Mechanics and Engineering,* vol. 174, pp. 171-190, 1999.

[10] X. Gao, R. Qiao and L. C. Brinson, "Phase Diagram Kinetics for Shape Memory Alloys: a Robust Finite Element Implementation," *Smart Materials and Structures,* vol. 16, pp. 2012-2115, 2007.

[11] H. Prahled and I. Chopra, "Comparative Evaluation of Shape Memory Alloy Constitutive Models with Experimental Data," *Journal of Intelligent Material Systems and Structures,* vol. 12, pp. 383-395, 2001.

[12] H. Sayyaadi, M. R. Zakerzadeh and H. Salehi, "A Comparative Analysis of Some One-Dimensional Shape Memory Alloy Constitutive Models Based on Experimental Tests," *Scientia Iranica B,* vol. 19, no. 2, pp. 249-257, 2012.

[13] K. Tanaka, "A Thermomechanical Sketch of Shape Memory Effect: One-Dimensional Tensile Behavior," *Res Mechanica,* vol. 2, no. 3, pp. 59-72, 1986.

[14] C. Liang and C. Rodgers, "One-Dimensional Thermomechanical Constitutive Relations for Shape Memory Materials," *Journal of Intelligent Materials, Systems, and Structures,* vol. 1, pp. 207-234, 1990.

[15] L. Brinson and M. Panico, "Comments to the paper "Differential an Integrated Form Consistency in 1-D Phenomenological Models for Shape Memory Alloy Constitutive Behavior",," *International Journal of Solids and Structures,* vol. 46, pp. 217-220, 2009.

[16] M. Elahinia and M. Ahmadian, "An Enhanced SMA Phenomenological Model: I. The Shortcomings of the Existing Models," *Smart Materials and Structures,* vol. 14, pp. 1297-1308, 2005.

[17] M. Elahinia and M. Ahmadian, "An Enhanced SMA Phenomenological Model: II. The Experimental Study," *Smart Materials and Structures,* vol. 14, pp. 1309-1319, 2005.

[18] L. Brinson, "One-dimensional Constitutive Behavior of Shape Memory Alloys: Thermomechanical Derivation with Non-constant Material Funstions and Redefined Martensite Internal Variable," *Journal of Intelligent Materials, Systems, and Structures,* vol. 4, pp. 229-242, 199.

[19] L. Li, Q. Li and F. Zhang, "One-Dimensional Constitutive Model of Shape Memory Alloy with an Empirical Kinetics Equations," *Journal of Metallurgy,* vol. 2011, no. 563413, pp. 1-14, 2011.

[20] K. Ikuta, M. Tsukamoto and S. Hirose, "Mathematical Model and Experimental Verification of Shape Memory Alloy for Designing Micro Actuator," in *Micro Electro Mechaical Systems (MEMS '91) Proceedings. An investigation of Micro Structures, Sensors, Actuators, Machines, and Robots*, Nara, 1991.

[21] Y. Ivshin and T. Pence, "A Thermomechanical Model for a One Variant Shape Material," *Journal of Intelligent Material Systems and Structures,* vol. 5, pp. 455-473, 1994.

[22] D. Madill and D. Wang, "Modeling and L2-Stability of a Shape Memory Alloy Position Control System," *IEEE Transactions on Control Systems Technology,* vol. 6, no. 4, pp. 473-481, 1998.

[23] T. R. Lambert, A. Gurley, K. Kubik, D. Beale and R. Broughton, "Numerical Heat Transfer Modelling of SMA Actuators and Controller Comparison," in *ASME Conf. on Smart Materials, Adaptive Structures, and Intelligent Systems*, Snowbird, 2017.

[24] J. Crews and R. Smith, "Quantification of Parameter and Model Uncertainty for Shape Memory Alloy Bending Actuators," *J. Intelligent Material Systems and Structures,* vol. 25, no. 2, pp. 229-245, 2014.

[25] M. Elahinia and H. Ashrafiuon, "Nonlinear Control of a Shape Memory Alloy Actuated Manipulator," *Journal of Vibration and Acoustics (Transactions of the ASME),* vol. 124, pp. 566-575, 2002.